

Look Before You Leap: Safe Model-Based Reinforcement Learning with Human Intervention

Yunkun Xu^{1,2}, Zhenyu Liu^{1,*}, Guifang Duan¹, Jiangcheng Zhu², Xiaolong Bai², Jianrong Tan¹

¹State Key Laboratory of CAD&CG, Zhejiang University

²Huawei Cloud

{xuyunkun, liuzy, gfduan, egi}@zju.edu.cn, {zhujiangcheng, baixiaolong1}@huawei.com

Abstract: Safety has become one of the main challenges of applying deep reinforcement learning to real world systems. Currently, the incorporation of external knowledge such as human oversight is the only means to prevent the agent from visiting the catastrophic state. In this paper, we propose MBHI, a novel framework for safe model-based reinforcement learning, which ensures safety in the state-level and can effectively avoid both "local" and "non-local" catastrophes. An ensemble of supervised learners are trained in MBHI to imitate human blocking decisions. Similar to human decision-making process, MBHI will roll out an imagined trajectory in the dynamics model before executing actions to the environment, and estimate its safety. When the imagination encounters a catastrophe, MBHI will block the current action and use an efficient MPC method to output a safety policy. We evaluate our method on several safety tasks, and the results show that MBHI achieved better performance in terms of sample efficiency and number of catastrophes compared to the baselines.

Keywords: Safety RL, Model-based RL, Model Predict Control

1 Introduction

Deep reinforcement learning (DRL) is proposed as an automated framework for intelligent decision-making problems, and has shown tremendous progress in various domains such as video games [1, 2], board games [3, 4] and robotic control [5, 6]. However, most of these success were achieved in the idealized simulator where agents can interact with the environment without restriction. In real-world applications, random exploration may lead to equipment damage or even worse results [7]. Consequently, when applied in the real world, DRL algorithms need to ensure the security throughout the whole learning process, especially in safety-critical scenarios.

This has encouraged the research on safety in DRL, which aims to maximize the cumulative rewards while minimizing safety violations during the training processes [8, 9]. Safe RL can be divided into two categories: trajectory-based [9, 10, 11] and state-based [12, 13, 14]. The former uses the cost function to evaluate the safety of the whole trajectory, while state-based methods place restrictions on a state-wise basis. Safe RL algorithms such as CPO [10] and HIRL [12] have shown that it is possible to significantly reduce the number of constraint violations in safety-critical tasks.

Unfortunately, most of existing methods have high sample complexity, which means that a large number of interactions with the real world are required, resulting in the increase of the number of catastrophe. Another shortcoming is that most of existing approaches use the explicitly defined constraint or safety cost function, while safety is subjective and always vague. For example, in autonomous driving, the overseer brakes when he judges that the car is going to crash. The overseer makes judgement based on subjective feelings rather than vehicle dynamic model. Finally, it is more strict and natural

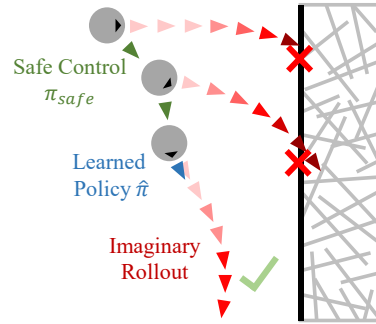


Figure 1: Imaginary safety detection and replacement of catastrophic actions in MBHI.

*Corresponding author

to define safety over the state. However, most of existing state-based methods are hard to effectively avoid potential disasters in the future [12, 13, 15], or need suboptimal demonstrations [14, 16].

To address the above-described challenges, in this paper, we introduce a novel safety-aware model-based framework, called Safe Model-based Reinforcement Learning with Human Intervention (MBHI), which incorporates safe RL with model-based methods and human knowledge. Intuitively, before excuting an action, people will estimate potential dangers in the future. In MBHI, an ensemble of deep neural networks is used to model a supervised Blocker to imitate the human overseer or explicit constraints, output the catastrophe probability of the state and evaluate the model uncertainty. As shown in Figure 1, at each time step, we roll out a trajectory with a certain number of steps in the learned dynamics to check the safety of the agent in the future. If dangerous, the MPC controller will take over and output a safe action to avoid possible future catastrophes in advance. Furthermore, safe active learning is integrated to enable grounded exploration only in safe regions, thereby accelerating model training on the premise of safety.

To summarize, the primary contributions of our work are as follows: (1) a novel safe model-based RL framework with human intervention, (2) safe active learning mechanism that only encourages agents to explore in safe regions, (3) a state-based action correction mechanism that perceive possible catastrophes in the future and avoid them in advance, (4) efficient MPC solving method that outputs a safe alternative policy in continuous action space.

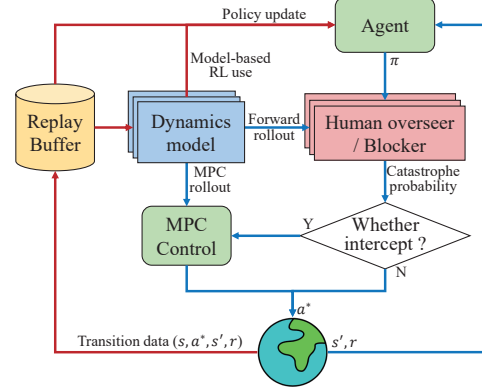


Figure 2: Overall framework of MBHI. The interaction phase is shown in blue and the policy learning in red.

2 Related Work

Safe RL: An interaction process is called safe if the agent rarely accesses the dangerous state [9, 11, 13]. Introducing external knowledge is the only way to ensure safety [12, 17]. Recently, various kinds of explicit constraints are used to impose some form of safety measures. To name some, constraints on expectation [9, 10], constraints on uncertainty [7, 18], and Conditional Value-at-Risk [11, 19, 20]. Unlike the above trajectory-based safety guarantees, [13] and [21] solve an optimization problem in the policy-level to ensure the safety of states. CARL [22] first trains the agent in non-safety-critical environments, and then adapts to the target environment. In the setting of implicit constraints, HIRL [12] and [15] train a supervised learner to imitate the human's intervention decisions and use it to evaluate the safety of the current state-action pairs. DDPGfD [16] and SAVED [14] learn the policy efficiently and safely in the sparse reward environment by using suboptimal human demonstrations. This work also focuses on learning implicit safety constraints from human knowledge. The main difference of MBHI is that (1) we image in the leaned dynamics to avoid potential hazards in the future, (2) the human knowledge only contains the judgment about catastrophes, not suboptimal demonstrations, and (3) non-safety-critical source environments are not available.

Model-based RL: Model-based RL exhibits low sample complexity and fast convergence. The learned dynamics model can be used for planning [4, 23], value expansion [24, 25], or imaginary training [26, 27, 28]. In planning approaches, MBMF [29] and PETS [23] use Model Predictive Control (MPC) to select actions based on the learned model. MVE [25] and STEVE [24] incorporate value expansion to improve the targets for temporal difference learning. ME-TRPO [26] and MBPO [27] are directly trained on imaginary data to accelerate policy learning. To limit the influence of the model error, the uncertainty estimation is widely used in MBRL. For instance, PETS [23] use uncertainty-aware models for trajectory propagation and planning. STEVE [24] interpolates between different imaginary rollout lengths to favor those targets with lower uncertainty. M2AC [30] uses the masking mechanism to only use the model when the model error is small.

In this work, STEVE is used as the base learning algorithm, but our framework is generally applicable to other model-based algorithms with uncertainty quantification, such as MBPO, M2AC, etc. We choose STEVE for three main reasons. Firstly, it explicitly estimates uncertainty for both dynamics and Q-function. Secondly, if the dynamics model cannot be learned or the Q-value network converges better, STEVE can reduce to model-free algorithm instead of learning from inaccurate imaginary data. Thirdly, since STEVE is an off-policy algorithm, the safety detection process in MBHI can be integrated with value expansion at each time-step to reduce calculation amount.

3 Preliminaries

3.1 Markov Decision Processes

We focus on Markov Decision Process (MDP) with continuous states and action spaces, defined as $(\mathcal{S}, \mathcal{A}, R, p_0, T, \gamma)$, in which \mathcal{S} is the state space, \mathcal{A} is the action space, $R : \mathcal{S} \times \mathcal{A} \times \mathcal{S} \rightarrow \mathbb{R}$ is the reward function, $p_0 : \mathcal{S} \rightarrow \mathbb{R}_+$ is the initial state distribution, $T : \mathcal{S} \times \mathcal{A} \rightarrow \mathcal{S}$ is the dynamics function, and $\gamma \in [0, 1]$ is the discount factor. The agent starts from an initial state $s_0 \sim p_0$, at each time step, the agent chooses an action $a_t \in \mathcal{A}$ in state $s_t \in \mathcal{S}$ according to a policy $\pi_\theta(s_t)$ parameterized with θ , transitions to a successor state $s_{t+1} = T(s_t, a_t)$ and receives a reward $r_t = R(s_t, a_t, s_{t+1})$. The goal of reinforcement learning is to find an optimal policy π_{θ^*} that maximize the expected discounted sum of rewards $\theta^* = \arg \max_\theta \mathbb{E}_{s_0 \sim p_0} [\sum_{t=0}^{\infty} \gamma^t r_t]$.

3.2 Stochastic Ensemble Value Expansion

In model-based RL, the agent learns the world model from the replay buffer to approximate the true dynamics function. In STEVE, the dynamics model consists of the following modules:

$$\begin{aligned} \text{Transition model : } s_t &\sim \hat{T}_\xi(s_t|s_{t-1}, a_{t-1}) \\ \text{Reward model : } r_t &\sim \hat{R}_\phi(r_t|s_t, a_t, s_{t+1}) \\ \text{Termination model : } d_t &\sim \hat{D}_\psi(d_t|s_t, a_t, s_{t+1}). \end{aligned} \quad (1)$$

An ensemble of parameters is maintained to estimate uncertainty in the learned dynamics (i.e. $\xi = \{\xi_i\}_{i=1}^{N_T}$, $\phi = \{\phi_i\}_{i=1}^{N_R}$, $\psi = \{\psi_i\}_{i=1}^{N_D}$). The entire dynamics model is optimized as follows:

$$\min_{\xi, \phi, \psi} \mathbb{E}[\|s_{t+1} - \hat{T}_\xi(s_t, a_t)\|^2 + \|r_t - \hat{R}_\phi(s_t, a_t, s_{t+1})\|^2 + \mathbb{H}(d_t, \hat{D}_\psi(s_t, a_t, s_{t+1}))], \quad (2)$$

where \mathbb{H} is the cross-entropy, and the expectation is calculated over data $\{(s_t, a_t, s_{t+1}, r_t, d_t)\}$.

For actor-critic methods or Q-learning methods, action-value function \hat{Q}_φ is a critical quantity to guide policy updating. The Temporal-Difference target is written as:

$$T^{TD}(r_t, s_{t+1}) = r_t + \gamma(1 - d_t)\hat{Q}_{\varphi^-}(s_{t+1}, \pi_\theta(s_{t+1})), \quad (3)$$

where φ^- means target network. STEVE improves TD targets by combining the short-term value estimate using the dynamics and long-term value estimate using \hat{Q}_φ . An ensemble of Q-functions is also maintained to evaluate the relative uncertainty between the dynamics and Q-function. Through these uncertainty estimates, STEVE dynamically interpolates between imagined rollouts of different horizon lengths, favoring those candidate targets with lower uncertainty, and give up utilizing them when significant errors are introduced. Thus, the interpolated target T_H^{STEVE} is written as

$$T_H^{STEVE}(r_t, s_{t+1}) = \sum_{h=0}^H T_h^\mu \cdot (T_h^{\sigma^2})^{-1} / \sum_j (T_j^{\sigma^2})^{-1} \quad (4)$$

$$T_h(r_t, s_{t+1}) = r_t + \sum_{i=1}^h D_i \gamma^i \hat{R}_\phi(s_{t+i}, a_{t+i}, s_{t+i+1}) + D_{h+1} \gamma^{h+1} \hat{Q}_{\varphi^-}(s_{t+h+1}, a_{t+h+1}), \quad (5)$$

where $D_i = d_t \cdot \prod_{j=1}^i (1 - \hat{D}_\psi(s_{t+j}, a_{t+j}, s_{t+j+1}))$, $s_{t+h+1} = \hat{T}_\xi(s_{t+h}, a_{t+h})$. T_h is the value expansion target with length h , T_h^μ and $T_h^{\sigma^2}$ are the empirical mean and variance for each T_h . If the environment is too complex or noise, STEVE will ignore the dynamics and reduce to model-free algorithm immediately.

4 Methods

In this section, we present a novel model-based safe RL framework, MBHI, as shown in Figure 2. In the interaction phase, at each time-step, we use the current policy network π_θ to roll out multiple steps in the learned dynamics, and check the safety of the imaginary trajectories with the supervised Blocker. If the catastrophe probability of the imaginary future rollout is greater than the threshold, the output action will be intercepted and replaced by the MPC controller. In policy learning phase, the model-based method is used to update the policy. Moreover, to overcome catastrophic forgetting problem of the network [12], we split replay buffer into safe and unsafe categories.

4.1 Catastrophe Prediction Network

Similar to HIRL [12], a supervised learner is trained to imitate the human overseer and block actions that are unsafe, but we maintain an ensemble of parameters for the Blocker $\mu = \{\mu_i\}_{i=1}^{N_B}$ to evaluate the uncertainty. In concrete terms, the human-imitator method has the following advantages. 1) Blocker can learn from data logs, human intervention data or explicit safety constraints by supervised learning. 2) Blocker is modular, it can be applied in distributed system and different tasks. 3) As binary network, the output value of the Blocker can be regarded as the distribution distance between the input state and the catastrophe zone. 4) Blocker can provide gradient information.

During human oversight phase, we store $(s_t, a_t, s_{t+1}, r_t, d_t, c_t)$ at each time-step, where c_t is a binary label for whether the current state is dangerous defined by humans. Thus, the Blocker can be trained in a supervised manner by minimizing the cross entropy loss as:

$$\mathcal{L}_{\mu_i} = \mathbb{H}(c_t, \hat{B}_{\mu_i}(s_t, a_t, s_{t+1})) \quad 1 \leq i \leq N_B. \quad (6)$$

Each \hat{B}_{μ_i} is initialized with various weights and trained on different input sequences. At this stage, for model-based RL, the collected data can also be used to train the dynamics using Eq (2). For the sake of fairness, in all experiments, we did not pre-train the dynamics model during the human oversight phase.

4.2 Safe Active Exploration

In order to reduce model uncertainty, we aim to query those points with large entropy, or where the disagreement would be most reduced in a posterior model. In our settings, the dynamics model takes the form of ensemble, and the disagreement can be quantified by calculating the empirical variance across the output of each model. Therefore, the optimization objective can be written as:

$$\pi_\theta = \max[\mathbb{E}_{\tau \sim \pi_\theta} [\sum_{t=0}^T ((1-\lambda)r_t + \lambda c_a \sigma^2(\hat{T}_\xi(s_t, a_t)))]], \quad (7)$$

where c_a is the coefficient of the active learning reward and λ is a policy dependent weighting. The second term of Eq 7 can also be regarded as maximizing the differential entropy of the transition model. The model outputs is in the form of empirical Gaussian distribution, its differential entropy can be easily obtained, given by $H(x) = \frac{1}{2}(\ln(2\pi\sigma^2) + 1)$. Therefore, maximizing variance is equivalent to maximizing model entropy. It is also possible to maximize the variance of the predicted reward, as proposed in [31], but we find it perform poorly in the sparse reward environment.

However, for safe RL, we do not want agents to visit unsafe regions, even if these areas have greater uncertainty. A simple yet effective method is to mask the exploration reward near the dangerous area. The catastrophe probability predicted by the Blocker can be regarded as the distribution distance to the unsafe region. Thus, Eq (7) can be rewritten in the form of safety-aware.

$$\pi_\theta = \max[\mathbb{E}_{\tau \sim \pi_\theta} [\sum_{t=0}^T ((1-\lambda)r_t + \lambda c_a \sigma^2(\hat{T}_\xi(s_t, a_t))(1 - \mathbb{E}_\mu[\hat{B}_\mu(s_t, a_t, s_{t+1})])^\alpha)], \quad (8)$$

where the exponent α controls the masking rate. λ determines the level of exploration guided by the learned transition model, it should tend towards stability with the convergence of the policy and the full exploration of the environment. In this work, we use the uncertainty measure of the dynamics to adjust λ adaptively. Formally, λ is defined as $\lambda_{t+1} = \frac{\bar{\sigma}_t^2(\hat{T}_\xi(\tau))}{2 \cdot \max_k \bar{\sigma}_{k < t}^2(\hat{T}_\xi(\tau))}$, where $\bar{\sigma}_t^2$ denotes the mean variance. This restricts λ to $[0, 0.5]$ and make the exploration to be guided by the reward signal.

4.3 Replacement of Catastrophic Actions

Before the agent execute the action to the environment, a C step trajectory from current state is rolled out in each dynamics. The catastrophe probability of the imagination is computed as follows.

$$p = \max_{c \in C} \mathbb{E}_{i \sim N_B, j \sim N_T} [\hat{B}_{\mu_i}(s_{c-1}^j, \pi_{\theta}(s_{c-1}^j), \hat{T}_{\xi_j}(s_{c-1}^j, \pi_{\theta}(s_{c-1}^j))]. \quad (9)$$

If p is greater than the safety threshold, it is considered that the agent will have a disaster in a certain number of steps under the current policy, and it is necessary to replace the action in advance. In HIRL [12], the author selects the alternative action based on a lookup table or the logit score ranking. However, these methods are not suitable for continuous action space and "non-local" catastrophes. In this work, Model-Predictive Control is used as an expert to output safe actions. Given a state s_t , the MPC prediction horizon H and the action sequence $a_{t:t+H-1}$, each dynamics model is used to predict the resulting trajectories $\{(s_{t+i}, r_{t+i-1})\}_{i=1}^H$. At each timestep t , the MPC controller solves the following optimization problem

$$\max_{a_t, \dots, a_{t+H-1}} \sum_{h=0}^{H-1} \hat{r}_{MPC}(s_{t+h}, a_{t+h}, s_{t+h+1}) \quad s.t. \quad s_{t+h+1} = \hat{T}_{\xi}(s_{t+h}, a_{t+h}), \quad (10)$$

where \hat{r}_{MPC} is the MPC reward. There are two requirements of it. First, guide the agent complete the obstacle-independent task. Second, guide the agent away from the unsafe regions. In consequence, \hat{r}_{MPC} contains the predicted external reward and the predicted disaster probability. In addition, we further introduce a Leave-One-Out safety estimation to make MPC samples as far away from the unsafe region as possible. Given the unsafe dataset \mathcal{D}_{us} and the MPC sampled state s_{t+h} , the estimator is defined as $u_{t+h} = D_{KL}[p(\cdot | \mathcal{D}_{us} \cup s_{t+h}) || p(\cdot | \mathcal{D}_{us})]$. The value of u_{t+h} is close to zero, when $p(\cdot | \mathcal{D}_{us} \cup s_{t+h})$ and $p(\cdot | \mathcal{D}_{us})$ gradually match each other, which indicates that the sampled state is dangerous. Therefore, we aim to maximize $\sum_{h=1}^H u_{t+h}$ to keep the whole MPC sampled sequence away from danger. The MPC return can be formulated as

$$\hat{r}_{MPC}(s_{t+h}, a_{t+h}, s_{t+h+1}) = \mathbb{E}_{\phi}[\hat{R}_{\phi}(s_{t+h}, a_{t+h}, s_{t+h+1})] + \mathbb{E}_{\mu}[\hat{B}_{\mu}(s_{t+h}, a_{t+h}, s_{t+h+1})] + u_{t+h+1}. \quad (11)$$

Finally, the controller executes the first action a_t to the environment, advances to the next time-step, and recheck the safety of the agent.

To improve the efficiency and performance of MPC, especially in high-dimensional action space, as shown in Figure 3, the gradient of the dynamics is used to guide the update of CEM sampling distribution. Each iteration consists of three steps: (1) Sample action sequences from CEM sampling distribution, and calculate MPC return with Eq (11). (2) Fix the dynamics parameters, and update action sequences via gradient ascent method. (3) Update the parameters of CEM sampling distribution. The action replacement mechanism is summarized in algorithm 1 in Appendix A.

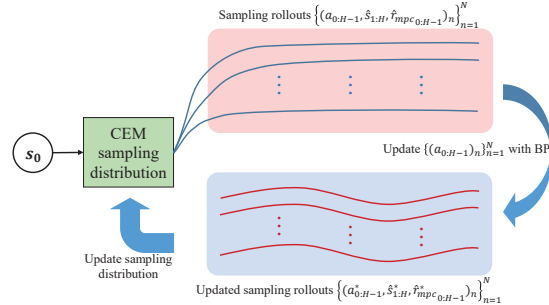


Figure 3: Schematic of MPC optimization method.

A negative reward must be given to guide the agent to learn a safe policy. The interception mechanism in MBHI considers the danger of the current policy in state s_t rather than the state-action pair. Thus, the negative reward should solely depend on the state. In this work, an intrinsic reward signal is generated based on how far the agent is from the unsafe region to encourage the agent to stay away from these areas. Specifically, the output of Blocker is served as this kind of measurement. Besides, to increase the punishment near the unsafe area, a boundary value *Bound* is introduced. When the predicted catastrophe probability is greater than this value, a larger scaling factor is used to increase the negative reward. The intrinsic reward signal is computed as

$$r^i(s_t, a_t, s_{t+1}) = \begin{cases} -c_l \mathbb{E}_{\mu}[\hat{B}_{\mu}(s_t, a_t, s_{t+1})] & \text{if } \mathbb{E}_{\mu}[\hat{B}_{\mu}(s_t, a_t, s_{t+1})] < Bound \\ -c_h \mathbb{E}_{\mu}[\hat{B}_{\mu}(s_t, a_t, s_{t+1})] & \text{else,} \end{cases} \quad (12)$$

where c_l and c_h are scaling factors, which control the penalties in different areas. *Bound* is the safety bound, a smaller bound will increase the complexity of the environment and obtain a more

conservative policy. Finally, the overall optimization problem can be written as

$$\theta^* = \arg \max_{\theta} \mathbb{E}_{a_t \sim \pi_{\theta}(s_t)} \left[\sum_{t=0}^{\infty} \gamma^t ((1 - \lambda)(r_t + r^i(s_t, a_t, s_{t+1})) + \lambda r^a(s_t, a_t, s_{t+1})) \right], \quad (13)$$

where r^a is the active learning reward in Eq (8). The full procedure is outlined in Algorithm 2 in Appendix A.

5 Experiments

5.1 Experiment Setting

In this section, we evaluate our approach and various baselines over five safety-critical continuous control tasks. 1) PuckWorld-L & PuckWorld-H: they differ in acceleration. The catastrophe of PuckWorld-H is locally avoidable, while PuckWorld-L is not. The agent is rewarded for reaching the target and is constrained to not touch the barrier. 2) Reacher: the agent is rewarded for reaching the target without touching the vertical bar. 3) Ant-Limit: the agent needs to move forward between two parallel barriers. 4) Ant-Block: the agent needs to move forward and avoid obstacles in the path. The last three tasks are adapted from PyBullet’s environments [32]. The visualization and details of these environments are given in Appendix B. All experiments are evaluated over 5 random seeds.

We compare our proposed MBHI against both the model-based and model-free baselines, PPO, DDPG and STEVE, and human intervention method, HIRL [12]. we extend HIRL to the continuous action space and also use STEVE as the basic algorithm. To ensure a fair comparison, HIRL and MBHI have the same Blocker and action replacement mechanism. HIRL also splits the replay buffer like MBHI. The final implementation differences between HIRL and MBHI are summarized as follows: (1) HIRL only receives a negative reward when a catastrophic action is blocked, while penalty is introduced in MBHI in the form of Eq (12); (2) HIRL does not employ active exploration; (3) HIRL does not image in the learned dynamics to detect potential disasters in the future. In all experiments, we use the same network structure of the policy, value, dynamics and Blocker for all algorithms, the number of ensemble models is 4. Details can be found in Appendix H.

5.2 Comparison of Performance

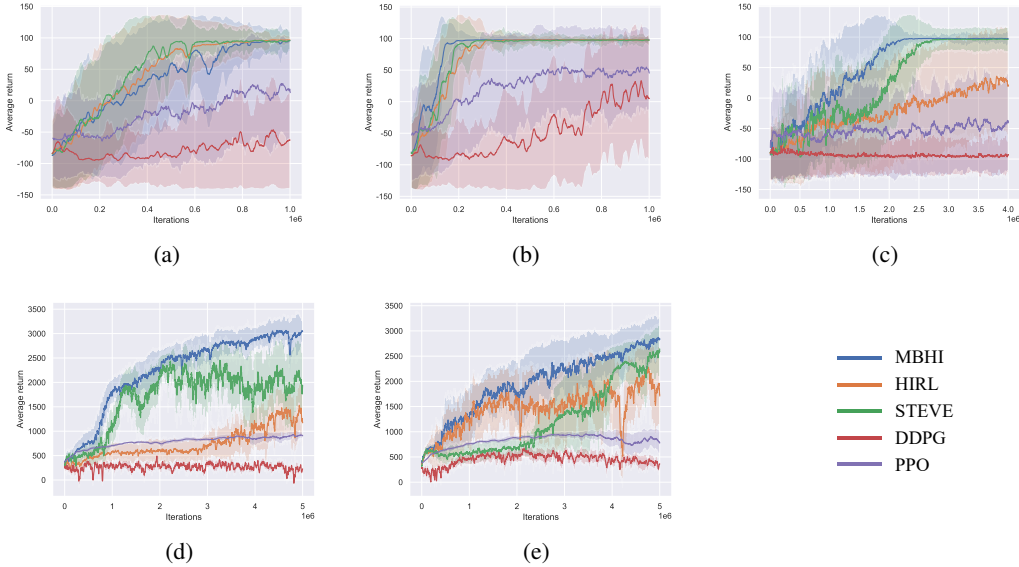


Figure 4: Learning curves of MBHI and baselines on five continuous control tasks over time (mean and standard deviation). (a) PuckWorld-L, (b) PuckWorld-H, (c) Reacher, (d) Ant-Limit, (e) Ant-Block. The x-axis is environment steps.

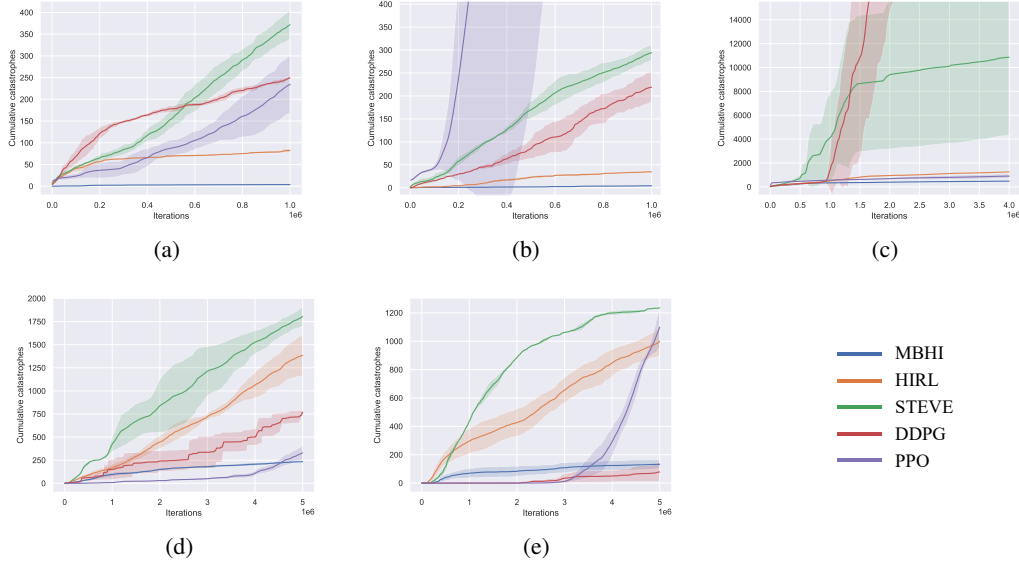


Figure 5: Cumulative catastrophes of MBHI and baselines on five continuous control tasks over time (mean and standard deviation). (a) PuckWorld-L, (b) PuckWorld-H, (c) Reacher, (d) Ant-Limit, (e) Ant-Block. The x-axis is environment steps.

The comparison results in Fig 4 demonstrate that the sample efficiency of MBHI is better than baselines, especially DDPG and PPO. MBHI achieves similar or better performances in all tasks than baselines. In PuckWorld-H, the parameters of MBHI and HIRL in safety inspection are exactly the same, but MBHI can converge faster, which illustrates the importance of active exploration. Frequent action shielding increases the complexity of policy learning. However, as an off-policy method, we do not find perceptible negative effects for MBHI.

The experiment results of STEVE and DDPG in Fig 5 demonstrate that optimal unsupervised behaviors can result in a large number of catastrophes. Note that DDPG and PPO has fewer catastrophes in some environments because the agent has not learned how to complete the task, and tends to move near the initial state. For example, in Ant-Block, the agent does not even successfully move to the place where it could encounter the obstacle, which can explain why the number of catastrophes of PPO suddenly rises in Fig 5e. Additionally, HIRL is able to successfully resolve locally avoidable catastrophes, but failed in other environments. By contrast, MBHI effectively avoids both "local" and "non-local" catastrophes during training. In the simple environment like PuckWorld, MBHI almost achieves zero catastrophes.

In tasks other than PuckWorld-H, HIRL cannot effectively save the agent. However, from Figure 5, we can see that the number of catastrophes in HIRL is significantly less than STEVE. This is because we divide the replay buffer in HIRL into safe and unsafe parts. Besides, we can also find that even though STEVE has converged, the number of catastrophes is still rising. Our findings are in line with recent results on catastrophic forgetting [12, 33]. MBHI can well restrain this problem.

5.3 Ablation on Safety Detection Rollout Length

Intuitively, the longer the safety detection distance, the more conservative the policy. We evaluate different safety detection rollout lengths on PuckWorld-L and PuckWorld-H. The result is shown in Figure 6. It shows that, surprisingly, when the safety detection distance is sufficient, our method is not so sensitive to the length of safety detection rollouts. This also proves that safety detection in the imagination can effectively avoid the catastrophe that will happen in advance. In addition, the long detection distance does not further reduce the cumulative catastrophes significantly, but it will introduce unnecessary calculation costs.

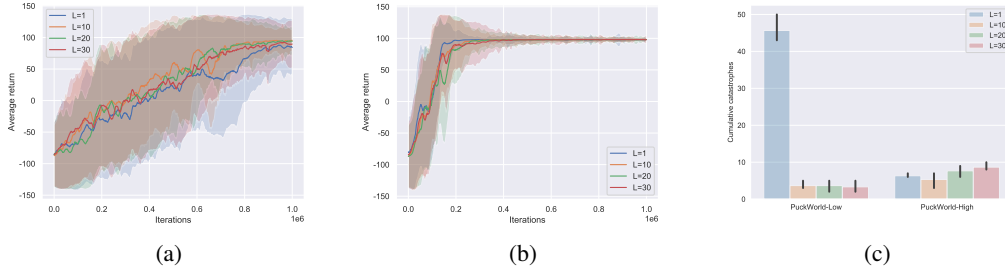


Figure 6: Ablation studies of the safety detection rollout length. (a) Average return in PuckWorld-L; (b) Average return in PuckWorld-H; (c) Cumulative catastrophes. Error bars are 95% bootstrap confidence intervals.

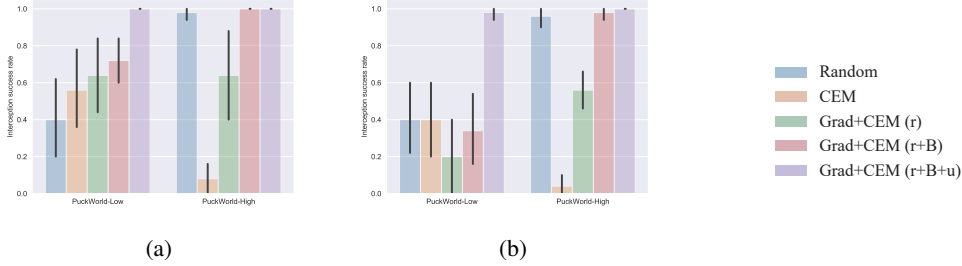


Figure 7: Interception success rate of different methods. (a) Converged dynamics model, (b) pre-trained dynamics model. For fair comparison, random shooting sampled 3200 times, CEM has 25 iterations of sampling 128 candidate actions, and Grad+CEM has 5 iterations plus 5 gradient steps of sampling 128 candidate actions. Shown is the mean performance, with error bars showing 95% bootstrap confidence intervals over 5 runs.

5.4 Comparison of Action Replacement Methods

We study the impact of different MPC optimization techniques and reward settings. The compared optimizers include the uniform random search [29] and the cross-entropy method [23]. The MPC reward settings include three types: 1) the reward \hat{r} predicted by the learned reward function; 2) \hat{r} and the catastrophe probability \hat{B} predicted by the Blocker; 3) \hat{r} , \hat{B} , and the distribution distance u between MPC samples and unsafe samples. For the sake of fairness, we also use $\hat{r} + \hat{B} + u$ as the MPC reward in Random and CEM. We sample ten points uniformly around the catastrophe as the initial position, and make the agent move toward the catastrophe at the fastest speed. In addition, the converged dynamics model and the pre-trained model are used as the simulator of MPC to evaluate the robustness of the proposed method. The results of the interception success rate are shown in Figure 7. It shows that our method has better interception performance and is more robust.

6 Conclusion

In this paper, we proposed a state-based safety oversight mechanism MBHI, which is based on the model-based RL algorithm with active learning method. MBHI is forward-looking, it considers the safety of the current policy in a certain time-step in the future, replaces dangerous actions in advance, and realizes the prevention of both "local" and "non-local" catastrophes. We evaluated the proposed algorithm on five continuous safety control tasks, the experiment results demonstrate that MBHI can significantly reduce catastrophes and accelerate training. Furthermore, our solution acts directly at the policy level, so it is independent of the learning algorithm and can be plugged into any existing model-based and model-free continuous control algorithms.

MBHI effectively alleviates the problem of "non-local" catastrophes, but it needs to have a certain understanding of the task. The safety detection distance needs to be long enough to avoid catastrophes in advance. Besides, hyperparameters are sensitive to the performance of the Blocker. Going forward, the safety detection length should be adaptive to the specific task, rather than set a fixed value. Moreover, in future research, we plan to study the theoretical guarantee of MBHI and improve

the algorithm’s robustness to the hyper-parameters. In terms of computation, since safety evaluation inevitably increases the cost of training process, we plan to study more effective methods to estimate the potential danger of the agent in the future and to integrate these estimates in model-based policy optimization.

Acknowledgments

This work was supported by the National Key Research and Development Program of China (grant No. 2019YFB1312600), National Natural Science Foundation of China (grant No. 52075480), Key Research and Development Program of Zhejiang Province (grant No. 2021C01008) and High-level Talent Special Support Plan of Zhejiang Province (grant No. 2020R52004).

References

- [1] S. Kapturowski, G. Ostrovski, J. Quan, R. Munos, and W. Dabney. Recurrent experience replay in distributed reinforcement learning. In *ICLR*, 2019.
- [2] V. Mnih, K. Kavukcuoglu, D. Silver, A. Graves, I. Antonoglou, D. Wierstra, and M. Riedmiller. Playing atari with deep reinforcement learning. *arXiv preprint arXiv:1312.5602*, 2013.
- [3] D. Silver, J. Schrittwieser, K. Simonyan, I. Antonoglou, A. Huang, A. Guez, T. Hubert, L. Baker, M. Lai, A. Bolton, et al. Mastering the game of go without human knowledge. *Nature*, 550(7676):354–359, 2017.
- [4] J. Schrittwieser, I. Antonoglou, T. Hubert, K. Simonyan, L. Sifre, S. Schmitt, A. Guez, E. Lockhart, D. Hassabis, T. Graepel, T. Lillicrap, and D. Silver. Mastering atari, go, chess and shogi by planning with a learned model. *Nature*, 588 7839:604–609, 2020.
- [5] T. P. Lillicrap, J. J. Hunt, A. Pritzel, N. Heess, T. Erez, Y. Tassa, D. Silver, and D. Wierstra. Continuous control with deep reinforcement learning. *arXiv preprint arXiv:1509.02971*, 2015.
- [6] D. Hafner, T. Lillicrap, J. Ba, and M. Norouzi. Dream to control: Learning behaviors by latent imagination. In *International Conference on Learning Representations*, 2020.
- [7] B. Lütjens, M. Everett, and J. How. Safe reinforcement learning with model uncertainty estimates. *2019 International Conference on Robotics and Automation (ICRA)*, pages 8662–8668, 2019.
- [8] J. Garcia and F. Fernández. A comprehensive survey on safe reinforcement learning. *J. Mach. Learn. Res.*, 16:1437–1480, 2015.
- [9] J. Fan and W. Li. Safety-guided deep reinforcement learning via online gaussian process estimation. *ArXiv*, abs/1903.02526, 2019.
- [10] J. Achiam, D. Held, A. Tamar, and P. Abbeel. Constrained policy optimization. In *International Conference on Machine Learning*, pages 22–31, 2017.
- [11] A. Cowen-Rivers, D. Palenicek, V. Moens, M. Abdullah, A. Sootla, J. Wang, and H. Ammar. Samba: Safe model-based & active reinforcement learning. *ArXiv*, abs/2006.09436, 2020.
- [12] W. Saunders, G. Sastry, A. Stuhlmüller, and O. Evans. Trial without error: Towards safe reinforcement learning via human intervention. In *AAMAS*, 2018.
- [13] G. Dalal, K. Dvijotham, M. Vecerík, T. Hester, C. Paduraru, and Y. Tassa. Safe exploration in continuous action spaces. *ArXiv*, abs/1801.08757, 2018.
- [14] B. Thananjeyan, A. Balakrishna, U. Rosolia, F. Li, R. McAllister, J. Gonzalez, S. Levine, F. Borrelli, and K. Goldberg. Safety augmented value estimation from demonstrations (saved): Safe deep model-based rl for sparse cost robotic tasks. *IEEE Robotics and Automation Letters*, 5:3612–3619, 2020.
- [15] B. Prakash, M. Khatwani, N. R. Waytowich, and T. Mohsenin. Improving safety in reinforcement learning using model-based architectures and human intervention. In *FLAIRS Conference*, 2019.
- [16] M. Vecerík, T. Hester, J. Scholz, F. Wang, O. Pietquin, B. Piot, N. Heess, T. Rothörl, T. Lampe, and M. A. Riedmiller. Leveraging demonstrations for deep reinforcement learning on robotics problems with sparse rewards. *ArXiv*, abs/1707.08817, 2017.

- [17] M. Alshiekh, R. Bloem, R. Ehlers, B. Könighofer, S. Niekum, and U. Topcu. Safe reinforcement learning via shielding. In *AAAI*, 2018.
- [18] G. Kahn, A. Villafior, V. H. Pong, P. Abbeel, and S. Levine. Uncertainty-aware reinforcement learning for collision avoidance. *ArXiv*, abs/1702.01182, 2017.
- [19] A. PrashanthL. Policy gradients for cvar-constrained mdps. In *ALT*, 2014.
- [20] Y. Chow, M. Ghavamzadeh, L. Janson, and M. Pavone. Risk-constrained reinforcement learning with percentile risk criteria. *ArXiv*, abs/1512.01629, 2017.
- [21] T. Pham, G. Magistris, and R. Tachibana. Optlayer - practical constrained optimization for deep reinforcement learning in the real world. *2018 IEEE International Conference on Robotics and Automation (ICRA)*, pages 6236–6243, 2018.
- [22] J. Zhang, B. Cheung, C. Finn, S. Levine, and D. Jayaraman. Cautious adaptation for reinforcement learning in safety-critical settings. In H. D. III and A. Singh, editors, *Proceedings of the 37th International Conference on Machine Learning*, volume 119 of *Proceedings of Machine Learning Research*, pages 11055–11065. PMLR, 13–18 Jul 2020. URL <https://proceedings.mlr.press/v119/zhang20e.html>.
- [23] K. Chua, R. Calandra, R. McAllister, and S. Levine. Deep reinforcement learning in a handful of trials using probabilistic dynamics models. In *NeurIPS*, 2018.
- [24] J. Buckman, D. Hafner, G. Tucker, E. Brevdo, and H. Lee. Sample-efficient reinforcement learning with stochastic ensemble value expansion. In *NeurIPS*, 2018.
- [25] V. Feinberg, A. Wan, I. Stoica, M. I. Jordan, J. E. Gonzalez, and S. Levine. Model-based value estimation for efficient model-free reinforcement learning. *ArXiv*, abs/1803.00101, 2018.
- [26] T. Kurutach, I. Clavera, Y. Duan, A. Tamar, and P. Abbeel. Model-ensemble trust-region policy optimization. In *ICLR*, 2018.
- [27] M. Janner, J. Fu, M. Zhang, and S. Levine. When to trust your model: Model-based policy optimization. In *NeurIPS*, 2019.
- [28] G. Kalweit and J. Boedecker. Uncertainty-driven imagination for continuous deep reinforcement learning. In *CoRL*, pages 195–206, 2017.
- [29] A. Nagabandi, G. Kahn, R. Fearing, and S. Levine. Neural network dynamics for model-based deep reinforcement learning with model-free fine-tuning. *2018 IEEE International Conference on Robotics and Automation (ICRA)*, pages 7559–7566, 2018.
- [30] F. Pan, J. He, D. Tu, and Q. He. Trust the model when it is confident: Masked model-based actor-critic. In *NeurIPS*, 2020.
- [31] P. J. Ball, J. Parker-Holder, A. Pacchiano, K. Choromanski, and S. Roberts. Ready policy one: World building through active learning. In *ICML*, 2020.
- [32] E. Coumans and Y. Bai. Pybullet, a python module for physics simulation for games, robotics and machine learning. <http://pybullet.org>, 2016–2019.
- [33] R. Kemker, A. Abitino, M. McClure, and C. Kanan. Measuring catastrophic forgetting in neural networks. In *AAAI*, 2018.
- [34] T. Schaul, J. Quan, I. Antonoglou, and D. Silver. Prioritized experience replay. In *ICLR*, 2016.

A Appendix: Algorithms

Algorithms 1 and 2 contain the pseudo-code of action replacement mechanism and complete optimization procedure in MBHI, respectively.

Algorithm 1 Action Replacement Mechanism in MBHI

- 1: **Inputs:** Initial state s_0 , MPC horizon H , number of CEM iterations T , number of gradient steps I , transition ensemble \hat{T}_ξ , reward ensemble \hat{R}_ϕ , Block ensemble \hat{B}_μ
 - 2: **for** $t = 0$ to $T - 1$ **do:**
 - 3: Sample K action sequences $\{a_{0:H-1}^{(t)}\}_{k=1}^K \sim \text{CEM}(\cdot)$
 - 4: **for** $i = 1$ to I **do:**
 - 5: Calculate imaginary rollouts $\{s_{1:H}^{(t)}\}_k = \hat{T}_\xi(\{a_{0:H-1}^{(t)}\}_k, s_0)$
 - 6: Calculate MPC returns for each action sequence by Eq (11)
 - 7: Update the action sequence $\{a_{0:H-1}^{(t)}\}_{k=1}^K$ via gradient ascent
 - 8: **end**
 - 9: Recalculate imaginary rollouts and MPC returns
 - 10: Update $\text{CEM}(\cdot)$ distribution with top N action sequences sorted by MPC returns
 - 11: **end**
 - 12: **Output:** The first action a_0^* from optimal action sequence $a_{0:H-1}^*$
-

Algorithm 2 Actual algorithm of MBHI

- 1: **Inputs:** Number of initial samples N_0 , interacting step T , length of safety detection H , safe threshold ε , scaling factors c_l and c_h , Block ensemble \hat{B}_μ
 - 2: **Initialize:** random initialize policy π_θ , value ensemble \hat{Q}_φ , transition ensemble \hat{T}_ξ , reward ensemble \hat{R}_ϕ , termination model \hat{D}_ψ
 - 3: Collect N_0 samples with random policy, initialize replay buffer $D = \{(s_t, a_t, r_t, s_{t+1}, d_t)\}_{t=1}^{N_0}$ and pre-train $\{\hat{T}_\xi, \hat{R}_\phi, \hat{D}_\psi\}$ N_0 times
 - 4: **for** each epoch **do:**
 - 5: Get initial state s_0
 - 6: **for** $t = 1$ to T **do:**
 - 7: Check the safety p_t of the current policy π_θ with Eq (9) in imaginary rollouts of depth H starting from state s_t
 - 8: **if** $p_t \geq \varepsilon$ **then** Compute action a_t using Algorithm 1
 - 9: **else** Compute $a_t \sim \pi_\theta(a_t|s_t)$ with policy network
 - 10: Execute a_t to the real world and add transition to D
 - 11: Train the dynamics model $\{\hat{T}_\xi, \hat{R}_\phi, \hat{D}_\psi\}$ on buffer D with Eq (2)
 - 12: Update π_θ and \hat{Q}_φ with model-based learning methods on buffer D with Eq (13)
 - 13: **end**
 - 14: **end**
-

B Appendix: Experiment Setup

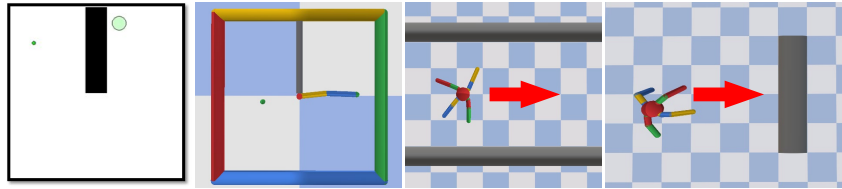


Figure 8: Visualization of the experimental environments. From left to right: PuckWorld, Reacher, Ant-Limit and Ant-Block.

- **PuckWorld-L:** A randomly generated puck has to reach a given random target in two-dimensional space. The maximum speed of the puck is 0.025, and the maximum acceleration is 0.002. Therefore, it needs to decelerate multiple steps in advance before the puck can stop. The constraint is that the puck cannot enter the black area in the middle. It's a catastrophe if the puck enters the black area.
- **PuckWorld-H:** Same as PuckWorld-L, except that the maximum acceleration is 0.025. It means that the puck can be stopped immediately. The catastrophe is the same as PuckWorld-L.
- **Reacher:** A two-link arm has to reach a given random target in two-dimensional space. The arm is not allowed to touch the vertical bar. It's a catastrophe if the arm collides with the vertical obstacle.
- **Ant-Limit:** An ant with four legs needs to run as fast as possible along the positive X-axis in three-dimensional space. The ant can only move between two parallel boundaries. It's a catastrophe if the ant's centroid crosses the boundary.
- **Ant-Block:** The basic environment is the same as Ant-Limit. The difference is that a vertical obstacle blocks the motion path of the ant. It's a catastrophe if the ant's centroid collides with the obstacle.

In PuckWorld and Reacher, 100 reward is given when the agent successfully reaching the target area, -100 when causing a catastrophe, and 0 in the rest of time. In Ant, -100 reward is given when the agent causing a catastrophe, and the reward is the same as the original environment Ant at other times. The episode will be terminated immediately if the agent violates the safety constraints.

C Appendix: Detailed Analysis of The Human Oversight Phase

In all experiments, only the obstacle was labeled as unsafe, which greatly reduces the workload of human labors (no need to deduce) and can quickly evaluate the proposed method. Since the input of the Blocker is (s_t, a_t, s_{t+1}) in practice, the transition can also be intercepted and labeled in advance. In this case, the labeled unsafe transition means that once it is visited, the agent cannot be rescued.

The human time-cost can be roughly formulated as follows [12]:

$$C = t_{human} \times N_{all}, \quad (14)$$

where C is the total time-cost of the oversight phase, t_{human} is the time-cost per human label, and N_{all} is the number of training samples. In our experiments, since the judgment of catastrophe is very simple, t_{human} is about 0.1 seconds. Therefore, the main way to reduce C is to reduce N_{all} . We fixed this problem through two methods. One is to shield the negative rewards for catastrophes from the environment to prevent the agent from quickly learning to avoid obstacles. The second is to initialize the agent near the obstacle with certain probability. Because the catastrophe is not complicated, the Human Oversight phase of PuckWorld and Reacher lasted for about 3 hours, and Ant lasted for about 5 hours. Finally, we believe that the available historical logs containing catastrophes will be able to effectively alleviate the problem of time-cost.

D Appendix: Visualization of The Parameter λ

The value of parameter λ defines the relative weighting of exploitation and exploration. With $\lambda = 0$ that training a policy only maximizes the expected return, and $\lambda = 1$ training a policy that only be encouraged to visit unfamiliar states. Fig 9 shows the plot of λ during policy training. In PuckWorld and Reacher, with the convergence of the policy and the full exploration of the environment, the value of λ gradually decreases to zero. While in Ant, λ does not converge to a small value, because the space in Ant is infinite, and Ant encourages the agent to walk as far as possible, instead of completing the task as soon as possible in a limited space. Therefore, during the training process, the agent in Ant is constantly visiting new states. We notice that the λ in Ant has a significant decrease in the initial of training. This is because the agent has not learned to move in the positive direction of X-axis, and has been walking near the origin, resulting in full exploration of this area.

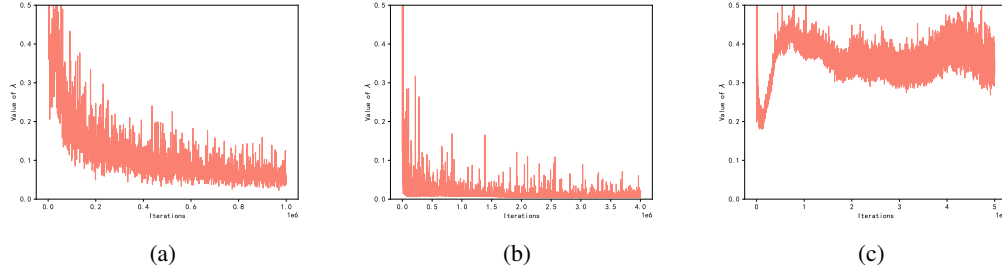


Figure 9: Visualization of the active learning parameter λ in Eq (13) during training. (a) PuckWorld, (b) Reacher, (c) Ant. The x-axis denotes the environment step.

E Appendix: Ablations

E.1 Scaling Factors

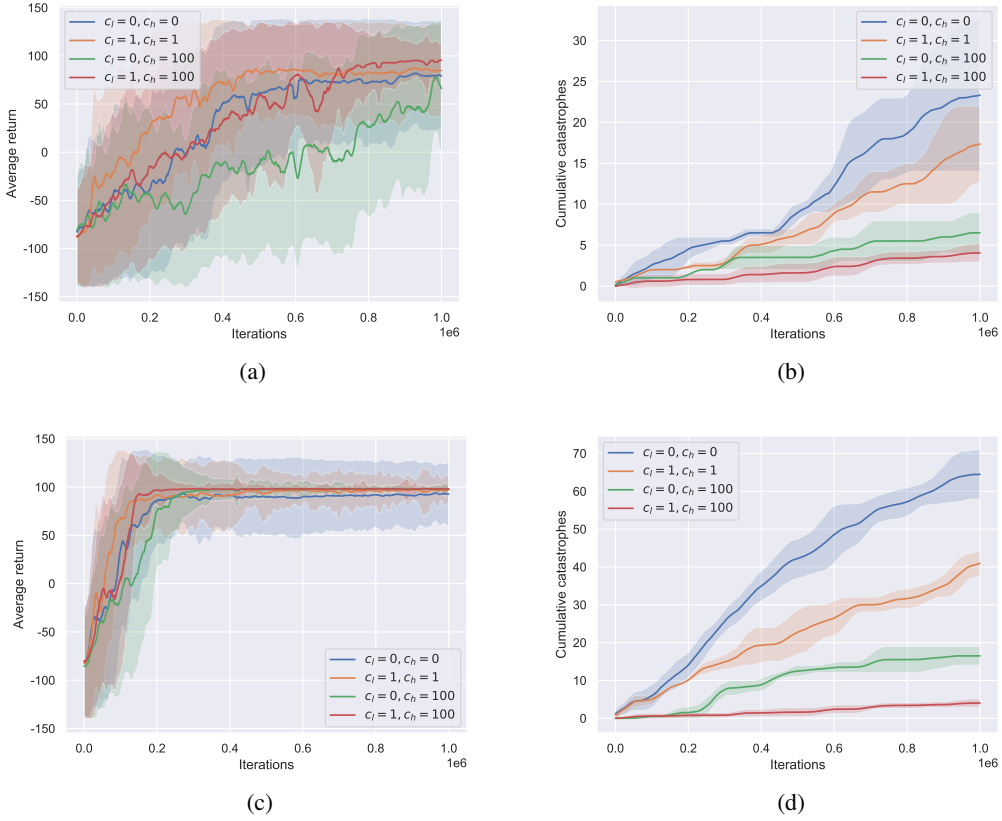


Figure 10: Evaluation of how scaling factors c_l and c_h affect MBHI performance in PuckWorld-L and PuckWorld-H. (a) and (b) are the performance and cumulative catastrophe of environment PuckWorld-L. (c) and (d) are the learning curves and cumulative catastrophe of environment PuckWorld-H.

An ablation study is performed on scaling factors c_l and c_h in Fig 10. ($c_l = 0, c_h = 0$) means that when the agent’s action are intercepted by the Blocker, it cannot obtain a negative reward to perceive potential dangers. When the model is evaluated in the PuckWorld, ideally, there is about 25% probability that the agent will pass through the dangerous area, that is, the expectation of the cumulative reward is $\mathbb{E}[G] = \frac{3}{4} \times r_{target} + \frac{1}{4} \times r_{catastrophe} = 50$. But in practice, due to the Blocker’s prediction error, the agent will visit the dangerous area during the training process and

thus have the opportunity to learn about catastrophes. As shown in Fig 10a and Fig 10c, the learned policy’s performance is better than 50, but the standard deviation of the cumulative reward is larger than other ablations, and it cannot converge to the optimal policy.

When the scaling factor c_l or c_h is non-zero, the knowledge of catastrophes is introduced to the agent by means of intrinsic reward, and helps agent avoid dangerous areas. Furthermore, in sparse reward environment, this kind of intrinsic reward can also accelerate convergence. c_h controls the penalties of the area in the immediate vicinity of the catastrophe. We make c_h much larger than c_l , which can strongly correct the behavior of the agent near the unsafe region. As can be seen in Fig 10, larger c_h can further reduce the number of cumulative catastrophe in the training phase. However, the larger c_h also increases the complexity of the environment and makes policy learning more difficult.

E.2 Safety Bound

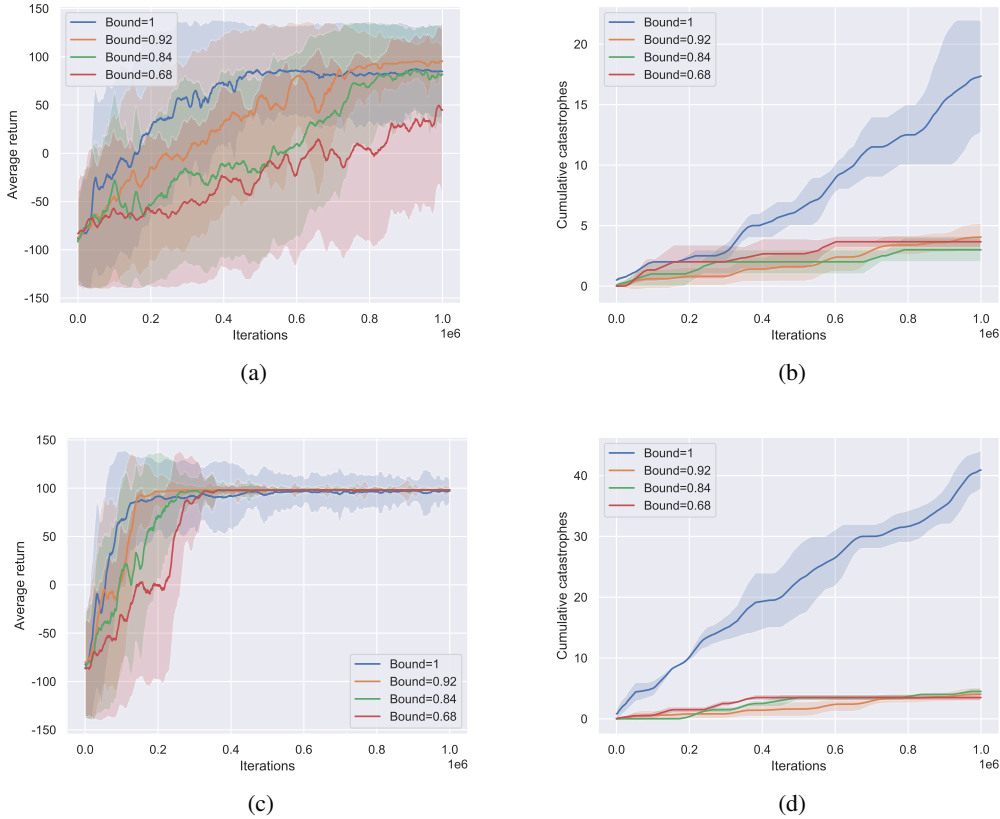


Figure 11: Evaluation of how safety bound affect MBHI performance in PuckWorld-L and PuckWorld-H. (a) and (b) are the performance and cumulative catastrophe of environment PuckWorld-L. (c) and (d) are the learning curves and cumulative catastrophe of environment PuckWorld-H.

We also conduct ablation studies about safety bound *Bound*, which are demonstrated together in Fig 11. *Bound* = 1 is equivalent to ($c_l = 1, c_h = 1$) described in Sec E.1. The introduction of the safety-aware intrinsic reward improves the sampling efficiency. However, due to insufficient punishment near the catastrophe, the agent will still occasionally try to cause catastrophes. From Fig 11c we can clearly find that the variance of *Bound* = 1 is much larger than other ablations, which means that it has not learned the optimal safety policy.

As shown in Fig 11a and 11c, as the value of *Bound* decreases, the speed of policy learning becomes slower and slower. This is because smaller *Bound* means the larger subjective disaster area (i.e. areas with large negative intrinsic reward). This will result in a reduction in the feasible state space of the agent, and increase the complexity of the task. As a consequence, the agent has to learn a

more conservative policy. Moreover, Fig 11b and Fig 11d indicate that too small *Bound* can not further reduce the number of catastrophe, but will greatly affect the speed of policy convergence.

F Appendix: Discussion of Safety-critical Components

In many natural scenarios, security constraints are subjective and difficult to be formulated explicitly. In addition, sub-optimal trajectories or demonstrations are not available, and humans can only judge whether the current state is safe or not. In this case, human-in-the-loop seems to be the only way to guarantee the safety of RL systems during training [12]. We studied whether the human-imitator could avoid both "local" and "non-local" catastrophes when enhanced with environmental dynamics approximators. As shown below, we summarize the key components to ensure safety:

- **Look before leap:** Imaging in the learning dynamics helps the agent to correct the catastrophic policy in advance. As shown in Fig 4, When the momentum of the agent in a certain direction cannot be decayed to zero immediately, it is necessary to block the dangerous action in advance. This is like the braking distance of a car. We must depress, hold down the brake pedal and turn the wheel in advance to avoid collisions.
- **Separated replay buffer:** Neural networks are always suffer from catastrophic forgetting [33], especially in reinforcement learning, where old samples are constantly replaced by new ones. Since there are very few unsafe samples compared with safe samples, it is easy to be forgotten. Splitting the replay buffer into safe and unsafe categories can effectively alleviate the problem of catastrophic forgetting by over-sampling unsafe samples. Similar to PER [34], importance-sampling method needs to be used to compensate the bias introduced by this prioritization.
- **Safety-aware intrinsic reward:** As presented in Appendix E, using the predicted catastrophe probability as an intrinsic reward can make the agent perceive the dangerous area during training. Furthermore, Larger intrinsic reward leads to a more secure and conservative policy, but makes the environment more complicated and the policy is more difficult to converge.
- **Model-based RL:** Model-based methods can significantly improve the sampling efficiency, so as to learn the safe policy faster. Moreover, the reward function and termination function in dynamics can also model the catastrophe from unsafe samples, thereby further improve the safety during policy learning. Besides, different from [7, 14, 18], approximating the environmental dynamics make the catastrophe prediction network only need to focus on the safety of the current state-action pair, rather than a sequence, making it easier to train.

G Appendix: Visualization of The Agent Motion

The visualization of interception points in environments PuckWorld-L and PuckWorld-H is shown in Fig 12. The interception region in PuckWorld-L is much larger than that in PuckWorld-H. In PuckWorld-L, due to the low acceleration and the long braking-distance of the agent, it is necessary to intercept dangerous actions multiple steps in advance. But, it is enough to replace dangerous actions one step ahead in PuckWorld-H.

As shown in Fig 12a, the interception points on the outside are significantly less than the areas close to the catastrophe. This is because the MBHI's interception strategy does not only depend on the current state, but also considers the current behavioral policy. Therefore, in the same state, with different behavioral policies, MBHI's interception results may also different. That is, if the agent's policy can avoid catastrophes by itself in the future, MBHI will not intercept it. In Fig 12, we also observe that there are more interception points at the lower end of the obstacle, mainly because it is more difficult to learn to bypass the obstacle than to avoid it.

The visualization of motion sequences is shown in Figure 13, MBHI executes the current behavioral policy in the imagination to decide whether to block the action.

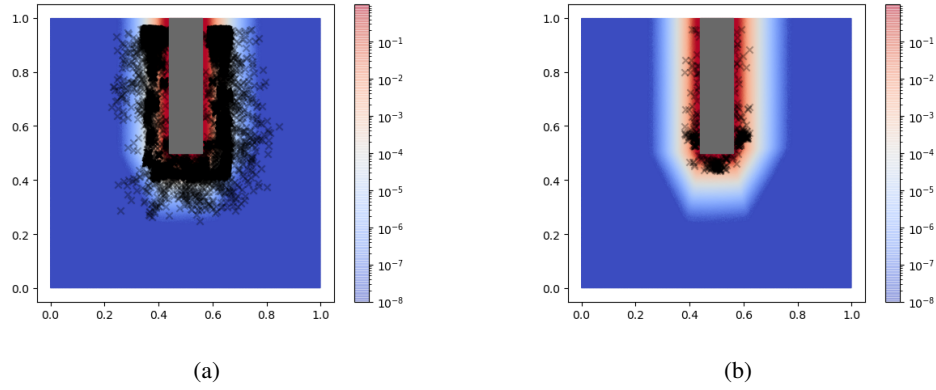


Figure 12: Visualization of state points intercepted by the Blocker. (a) PuckWorld-L, (b) PuckWorld-H. The gray rectangle indicates the obstacle, which is labeled as unsafe when training the Blocker. Red corresponds to a high probability of catastrophe predicted by the Blocker (normalized on a log scale), while blue to a lower.

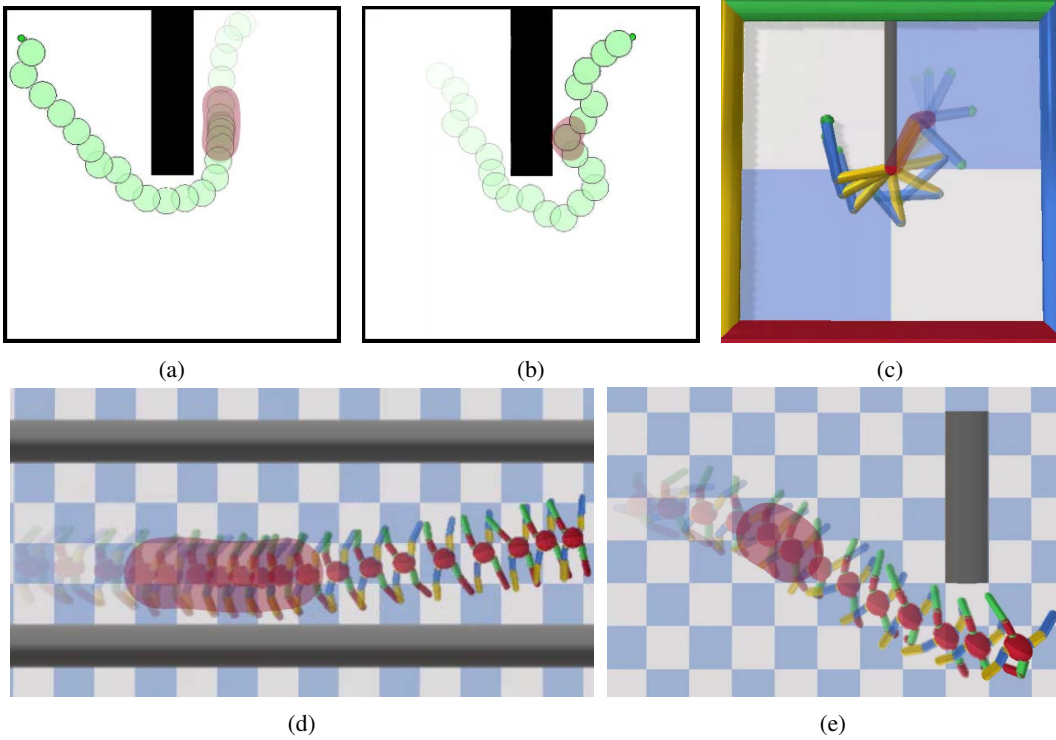


Figure 13: The Visualization of motion sequences in experiments. (a) PuckWorld-L, (b) PuckWorld-H, (c) Reacher, (d) Ant-Limit, (e) Ant-Block. The red area indicates that the action predicted by the agent's behavioral policy is blocked and replaced by the MPC controller. The final display is the safe trajectory monitored by the Blocker and corrected by MPC.

H Appendix: Implementation Details

In this work, we follow the same network structure and policy learning method as STEVE. All models are fully connected neural networks optimized by Adam with learning rate of $3e - 4$. The value network, policy network, reward model, termination model and Blocker each has 4 layers of size 128. The transition model has 8 layers of size 512.

The replay buffer size is $1e6$. The first $1e5$ frames are sampled by the agent interacting with the environment through random actions. After that, the dynamics model is pre-trained $1e5$ times, and then 1 model update and 1 policy update are performed for each frame sampled from the environment. The mini-batch size of all models is 512. We use soft update for the target network instead of hard update used in STEVE. Note that the replay buffer is divided into two parts, safe and unsafe, and sampled from them in equal proportions. This prioritization can introduce bias, which we correct with importance sampling method. When correcting the dangerous action by MPC controller, the Gradient + CEM method uses 5 iterations plus 5 gradient steps to sample 128 candidate actions.

The policy network and value network of DDPG and PPO are also fully connected neural networks with 4 layers of size 128. The hyper-parameters of DDPG are the same as STEVE, but there is no model ensemble and dynamics. For the hyper-parameters of PPO, the clipping parameter is set to 0.2, the GAE Lambda is selected as 0.95, the learning rate is $3e - 4$, and the mini-batch size is 512.

Table 1: Experiment hyper-parameters.

Hyperparameter Name	PuckWorld-Low	PuckWorld-High	Reacher	Ant-Limit	Ant-Block
Safety detection length	10	1	8	10	10
MPC horizon	10	10	10	10	10
Safety weight	1	1	1	1	1
Active learning coefficient	5e4	10	1e3	10	10
Safe threshold	0.96	0.96	0.96	0.99	0.99
Intrinsic reward bound	0.92	0.92	0.92	0.95	0.95
Scaling factor c_l	1	1	1	0.5	0.5
Scaling factor c_h	100	100	100	10	10